



ELSEVIER

Available online at www.sciencedirect.com

SCIENCE @ DIRECT®

Journal of Constructional Steel Research 61 (2005) 567–586

JOURNAL OF
CONSTRUCTIONAL
STEEL RESEARCH

www.elsevier.com/locate/jcsr

Response of a continuous, skewed, steel bridge during deck placement

Tze-Wei Choo^a, Daniel G. Linzell^{b,*}, Je Il Lee^b,
James A. Swanson^c

^a*McCormick, Taylor & Associates, Inc., Philadelphia, PA 19103, USA*

^b*Department of Civil and Environmental Engineering, Pennsylvania State University, State College, PA 16802, USA*

^c*Department of Civil and Environmental Engineering, University of Cincinnati, Cincinnati, OH 45221, USA*

Received 20 May 2004; accepted 26 October 2004

Abstract

An investigation was conducted to study environmental, material and deck placement effects on the behavior of a continuous, skewed, High Performance Steel (HPS), integral abutment bridge during construction using field data and three-dimensional finite element models. The finite element models were calibrated against girder strain measurements recorded during deck placement. During calibration, the effects of temperature changes during deck placement were clearly evident and were shown to have a significant effect on the accuracy of the finite element results. Effects from hardening of the concrete deck as the pour progressed were shown to be less evident. A calibrated model was used to compare stress variations and deflections of the two outer girders when concrete was placed (1) perpendicular to the girders and (2) parallel to the skew. The influence of various parameters on numerical model results was postulated and a deck placement method was recommended.

© 2005 Published by Elsevier Ltd

Keywords: Bridge; High performance steel; Skewed; Semi-integral; Construction; Deck; Continuous; Numerical; Experimental

* Corresponding author. Fax: +1 814 863 7304.
E-mail address: dlinzell@engr.psu.edu (D.G. Linzell).

1. Introduction

There is a growing demand for skewed steel bridges as the needs for complex intersections and the problems with space constraint in urban areas arise. Skewed bridges are useful when roadway alignment changes are not feasible or economical due to the topography of the site and also at particular areas where environmental impact is an issue. The effects of skew on the response of completed structures have been well documented, with effects being shown to be more significant for skew angles greater than 30° [1,2]. Critical values for vertical deflections and bending moments within in-service skewed bridges have been shown to be lower when compared against those in similar right bridges [3–7]. Conversely, torsional rotations, shears and moments have been shown to be larger for skewed bridges. In addition, studies have also demonstrated that interaction between main support girders and transverse bracing members (diaphragms and cross frames) influences skewed bridge load distribution due to an increase in torsional rotations at certain sections of the longitudinal girders [3–7]. Additional work has shown that the magnitude of torsional shear rotations at skewed bridge supports are largest at the obtuse corners [8].

While a number of studies dedicated to the response of in-service skewed bridges have been completed, as presented above, there are few studies that focus on the behavior of skewed bridges during construction. Torsional moments developed in steel bridges with large skews are difficult to predict during construction, as the alignment of the screed can result in an uneven distribution of wet concrete dead loads across the superstructure that increase the skew effects. There has been a lack of research studying the effects of the disproportionate distribution of dead loads on the superstructure during construction.

Coupled with the increase in the design and construction of skewed bridges has been an increase in the utilization of High Performance Steel (HPS) for bridge superstructure units and the use of integral or semi-integral abutments for the substructure. HPS offers improved toughness and weldability when compared to more conventional steels and, when produced with yield strengths of 70 or 100 ksi (482–689 MPa), it provides an attractive alternative to other materials for various bridge structures [9].

While HPS has been available for a number of decades, its utilization by the bridge industry has begun relatively recently, beginning with the construction of two bridges in Tennessee and Nebraska in the late 1990s [10,11]. Since these two initial projects, a number of other states, including Ohio, have recognized the economic benefits of using HPS and currently over 100 HPS bridges have been placed into service [12].

Along with the increased implementation of HPS bridge structures in the U.S., there has been an increase in research related to the development of improved design and fabrication criteria for these structures. This research has included: (1) development of improved production and welding techniques for HPS [13–15]; (2) experimental and numerical studies of HPS plate girder flexural strengths [16–18]; (3) development of procedures for optimal design of HPS bridges [10]; and (4) cost comparisons between HPS, conventional steel and concrete bridge designs [19]. However, there has been no published information to date related to the response of completed HPS bridges under loads induced during construction or while in service.

The use of semi-integral and integral abutments also continues to increase. For these kinds of structures, the superstructure and substructure are assumed to behave as a unit

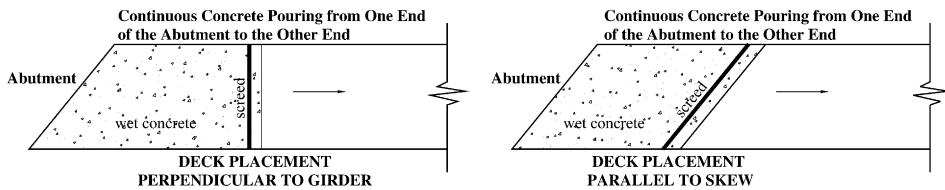


Fig. 1. Deck pour methods.

and expansion joints are eliminated. The girders act with the abutment and superstructure expansion is accommodated either through (1) an elastomeric pad placed underneath the abutment backwall for semi-integral abutments or (2) through movement of the entire abutment and foundation for integral abutments [20].

A large amount of research related to semi-integral and integral abutments has also been completed, with work predominantly focusing on: (1) characterization of interaction between substructure units and the supporting soil [21–23]; (2) development of analysis methods that predict stresses and deformations in superstructure and substructure units resulting from environmental, time-dependent and directly applied loads [24–28]; (3) development of design criteria and procedures [29–33]; and (4) examination and assessment of the performance of in-service integral abutment bridges [34–37]. While there have been a number of projects focusing on the qualitative examination of in-service semi-integral and integral abutment bridges, only a few studies have placed instrumentation onto actual structures and recorded their response and only two projects [38,39] have involved study of actual structural response during construction.

Therefore, this work attempts to add to the state-of-the-art related to skewed steel bridge response during construction by experimentally and numerically studying a continuous, skewed, HPS, semi-integral abutment bridge during placement of the concrete deck. Results from field monitoring of the structure during deck placement are compared to numerical predictions to ascertain influences of various parameters on behavior and alternative methods for placing the deck are examined.

2. Objectives

The objective of the research described herein was to study environmental, material and concrete placement effects on girder response in a recently constructed, skewed, HPS, semi-integral abutment bridge. The study examined stresses in the exterior plate girders of the bridge and compared those stresses to the field data.

The environmental and material studies examined the effects of air temperature changes during the pour and of setting of the concrete on forces developed in the superstructure. The accuracy with which numerical models predicted actual response when these effects were included or ignored is presented and discussed.

In addition, outer girder stresses were compared for two possible wet concrete placement schemes. The first was continuous placement of the wet concrete perpendicular to the girders, which was followed in the field, and the second was continuous placement of the wet concrete parallel to the skew (Fig. 1). The deck pour method that resulted in

the least detrimental response of the structure (i.e. lowest rotations and stresses) at the completion of the pour is identified and discussed.

3. Structure description

The structure that was studied is a four-span continuous, HPS bridge with semi-integral abutments that was recently constructed in Ohio. Fig. 2 details the framing plan and a typical cross section. Elastomeric bearings are located at Piers 1 and 3. Span lengths from south to north are 78'-5" (23.90 m), 130'-10" (39.88 m), 126'-10 $\frac{1}{2}$ " (38.67 m) and 82'-4 $\frac{1}{2}$ " (25.14 m) center to center of the bearings with a skew angle of 39°. Each girder is constructed with flanges ranging from 12" \times 7/8" (30.48 cm \times 2.2 cm) to 13" \times 2" (33 cm \times 5.1 cm). The web plate is 48" \times $\frac{1}{2}$ " (121.9 cm \times 12.7 cm). The girders are braced with cross frames containing 3 $\frac{1}{2}$ " \times 3 $\frac{1}{2}$ " \times 3/8" (8.9 cm \times 8.9 cm \times 0.95 cm) angles that are placed perpendicular to the webs as shown in Fig. 2. The girders are hybrid sections composed of HPS70W thermo-mechanical control process (TMCP) HPS flanges and ASTM A588/A709 Grade 50 webs. Cross frames were also constructed of Grade 50 steel and were arranged in an X-shaped pattern. The use of hybrid HPS sections resulted in reduced cross sectional dimensions compared with what would have occurred if standard steel plate was used for the flanges. It can be inferred that, as a result, the structure was more flexible than one that used Grade 50 steel everywhere and effects from varying concrete placement schemes on response would be more pronounced. However, other design decisions (e.g. semi-integral abutments) would also influence superstructure response during construction in a fashion that could make pour sequence effects less pronounced. It is the authors' opinion that, irrespective of the type of superstructure and substructure units that are designed, results discussed herein provide important information that should be considered during the design and construction of skewed, steel plate girder bridges.

The concrete deck was placed during a single seven-hour daytime pour initiating at the south abutment and proceeding to the north abutment. Retarders were placed into the concrete mix theoretically to prevent the concrete from setting until the pour was completed. A single screed was used for the pour and it was aligned so that the leading edge of the wet concrete would be placed perpendicular to the centerline of the roadway (case (a) from Fig. 1), as shown in Fig. 3.

4. Field monitoring

Nine Bridge Diagnostics, Inc., strain transducers were affixed to the exterior girder bottom flanges near their tips and on their webs approximately 3 $\frac{3}{4}$ " (9.53 cm) below the top flanges at locations G1A, G1B and G5A (Fig. 4) to obtain strain data during the pour. These gages recorded data at 2.5 min intervals throughout the deck placement process. Strains were converted to stresses assuming linear elastic behavior and stress variations during the deck pour were examined.

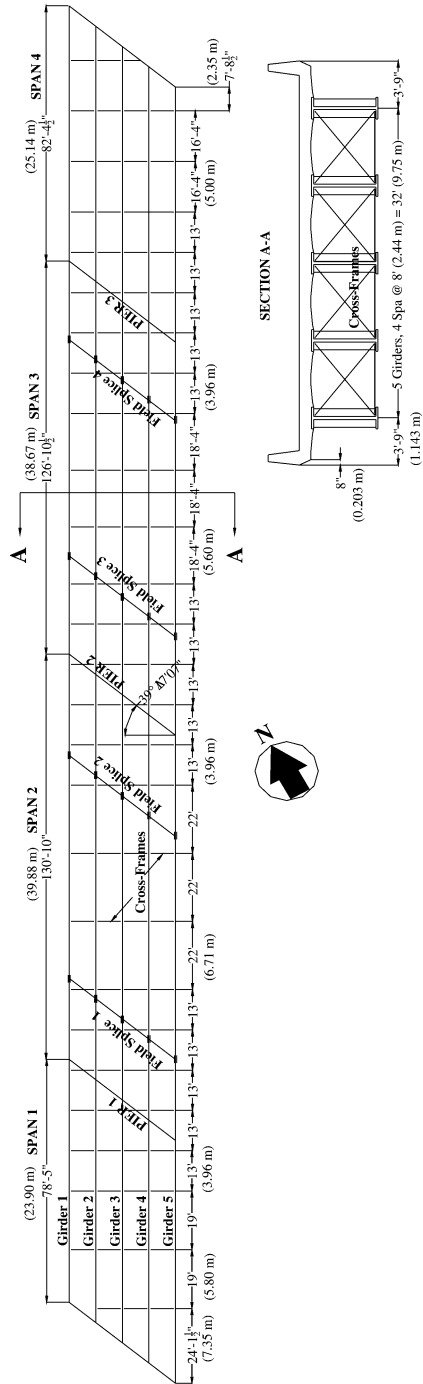


Fig. 2. The framing plan and a typical cross section.



Fig. 3. Deck pour orientation—perpendicular to the roadway centerline.

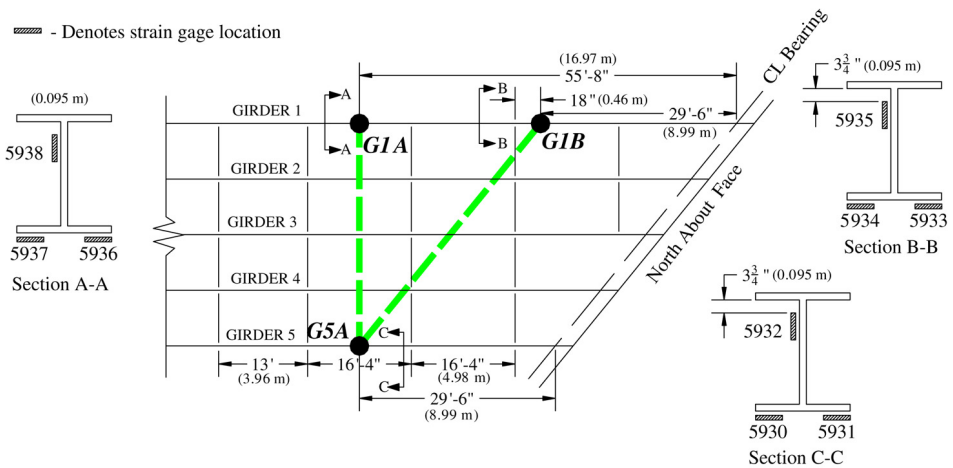


Fig. 4. Location of strain gages.

5. Numerical program

A three-dimensional finite element model was developed from the design plans using SAP2000 Version 8. SAP2000 was selected because it is commonly used by practitioners and Version 8 offers a feature for staged (incremental) construction analysis.

The model consists of the girders and wet concrete being represented using either three- or four-noded shell elements. All the girder shell elements are four-noded ones while the wet concrete elements consist of both three- and four-noded shells. Shell elements were selected for the deck to provide an accurate distribution of the concrete dead load to

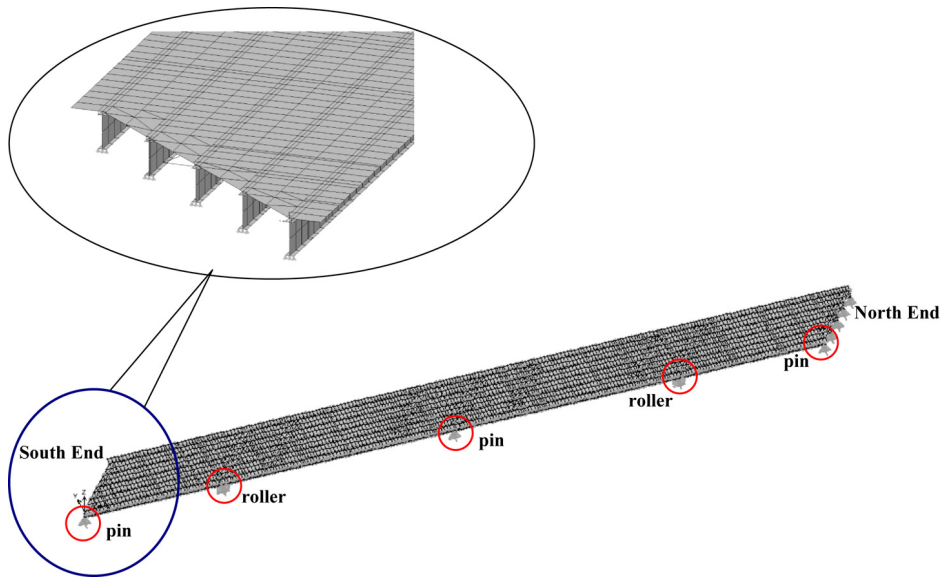


Fig. 5. The three-dimensional finite element model with final calibration boundary conditions.

the girders. Although it is understood that the use of four-noded shells provides a more accurate solution, since deck stresses were not examined three-noded shells were deemed acceptable for the deck. The shell elements were defined as elastic thin plates where the effect of transverse shear deformation was neglected.

Deck shell elements were connected to the girders using rigid links (frame elements) to transfer the wet concrete loads and to maintain compatibility between the deck and girders. Rigid link stiffness was established using a large modulus and a material density was assigned that would not contribute significantly to overall structure dead load. Three-dimensional frame elements were used for the cross frames. A detail depicting the model and indicating boundary conditions after calibration is shown in Fig. 5.

Loads placed onto the finite element model consisted of self-weights of the superstructure components (girders and cross frames) and the wet concrete. The model did not initially incorporate any additional loads caused by temperature changes that the structure experienced during the pour. In addition, any effects caused by setting of the concrete deck (i.e. change in deck stiffness) during the pour were not initially incorporated.

6. Model calibration

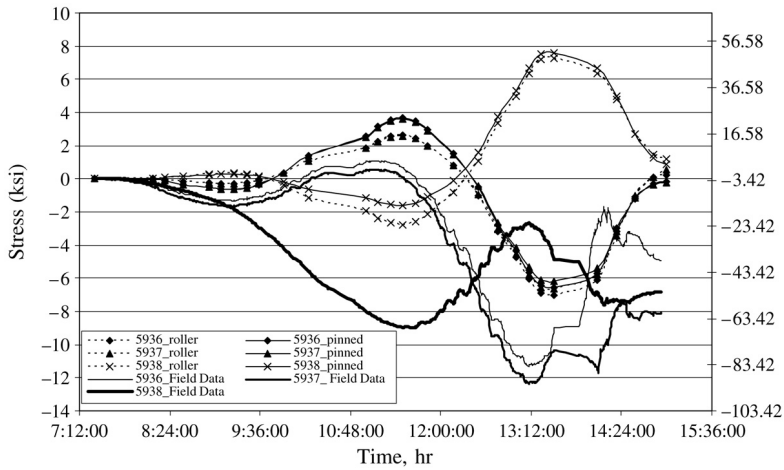
Stresses obtained from the finite element model were compared to measured values at strain gages on G1 and G5 (G1A, G1B and G5A; see Fig. 4) obtained during the deck pour. The finite element model had nodes located at the top of the web and, therefore, linear interpolation between nodes nearest to the transducer locations was used to perform any comparisons.

6.1. Boundary conditions

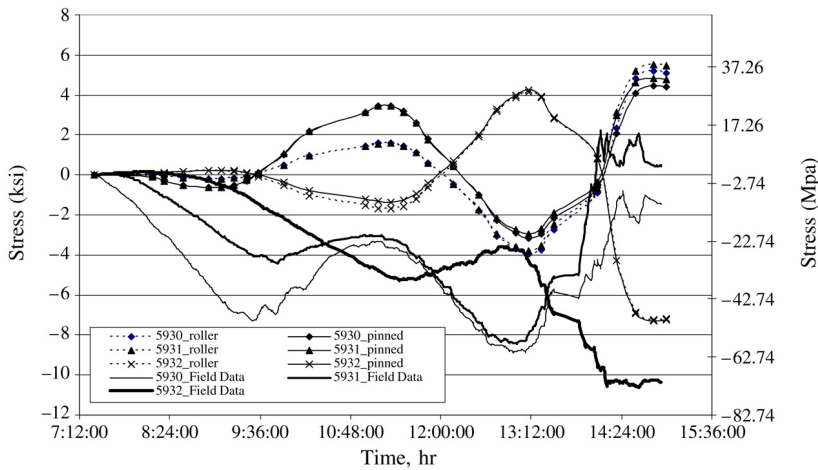
To accurately model the effects of the semi-integral abutments, detailed information regarding soil types and properties at the bridge site would need to be obtained. These properties would have helped establish the stiffness of the semi-integral abutments and the subsequent levels of restraint on the superstructure; however, insufficient information regarding actual soil conditions and properties was available. Examination of the field data indicated limited rotational restraint near the abutments. Therefore, girder abutment supports could initially be modeled using either rollers or pins. Girder response to deck placement for pinned abutment supports was considered to be one extreme for abutment restraint while roller supports were considered the other extreme. Finite element predictions for girder stresses at various instances during the deck pour were compared to field data to help assess which support conditions best mimicked actual behavior. Results from comparisons between measured and predicted flange stresses for the pinned and roller cases, plotted in Fig. 6(a) and (b) for G1A and G5A, are summarized in Table 1. The table gives girder stresses for various extremes measured during the pour and after it was completed. The extremes occurred between the 8th and 10th hour of the pour (Extreme 1), between the 11th and 12th hour (Extreme 2), between the 13th and 14th hour (Extreme 3). It was observed that the percentage differences at end of pour were highest at G1A, a location furthest from the abutment, followed by G1B, the location nearer to the acute corner. The least percentage differences at end of pour were at G5A, a location nearer to the obtuse corner. While percentage differences indicated in the table were in some cases quite large, relative magnitudes for these differences were generally quite small. In addition, when both the figures and the table were examined and compared to the field data, results were largely inconclusive regarding the clear selection of one boundary condition set (pinned or roller) over the other. Roller supports appeared to provide more accurate predictions of response at intermittent points during the pour while pinned supports provided more accurate predictions of response at some of the extremes and at the completion of the pour. Therefore, pinned supports were chosen for the remainder of the calibration steps and pour sequencing studies. It is understood that more accurate modeling of the actual boundary conditions, such as the incorporation of linear and/or nonlinear springs to mimic actual translational and rotational restraint at the semi-integral abutment, would influence the results. However, on the basis of the observed field data and boundary condition calibration work that was completed, the support condition influence on trends that were observed from the parametric studies discussed in the sections that follow was assumed not to significantly affect the trends and results that are reported herein.

6.2. Incorporation of temperature effects

Representative comparisons between numerical predictions for flange stresses from the finite element model with pinned supports against the field data during the pour are provided in Fig. 7(a) and (b). The figures indicate that, while the finite element models predicted trends for girder stresses quite well, as the pour progressed a general divergence between numerical and field results occurred. The field data generally experienced a



(a) G1A.



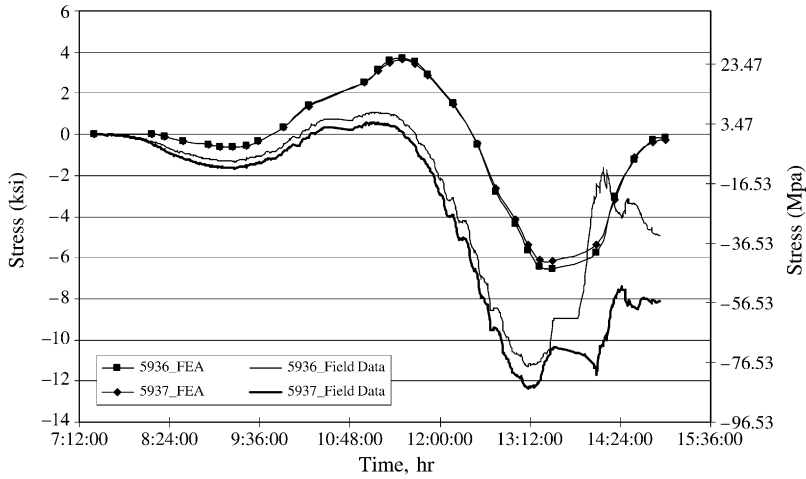
(b) G5A.

Fig. 6. Comparing girder stresses, for pinned and roller abutment supports.

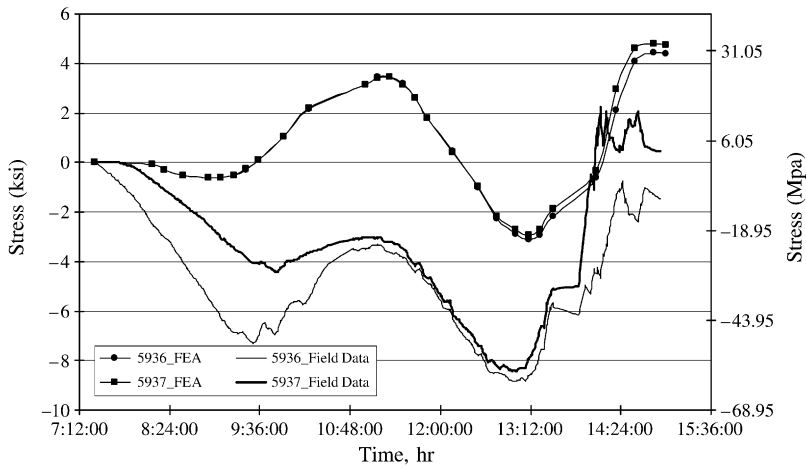
gradual shift towards compressive stresses at all gage locations and this shift was not reproduced in the model.

To attempt to improve model accuracy prior to examining deck placement effects on response, air temperature changes that occurred during the pour were incorporated into the model. Values were recorded along the eastern side of the north abutment during the entire pour and, as is shown in Fig. 8, the temperature varied from 36.0 °F (2.2 °C) to 63.7 °F (17.6 °C) during the seven-hour pour.

These temperature trends were incorporated into the finite element models by heating up the entire superstructure in a fashion that matched Fig. 8. Results from the analysis



(a) G1A.



(b) G5A.

Fig. 7. Experimental and numerical bottom flange stress variations, for G1 and G5.

including temperature and from the original analysis were again compared to the field data. Representative comparisons are shown in Fig. 9(a) and (b) for each girder. The results clearly indicate an improvement in the numerical predictions, with errors in stress predictions being reduced from about 103% to 3% on average in flanges.

6.3. Incorporation of concrete stiffness

An additional attempt at improving numerical model accuracy was made prior to examining deck placement effects through the incorporation of changes in concrete stiffness. The contractor used a Master Builders Pozzoloth 200 N retarder to prevent

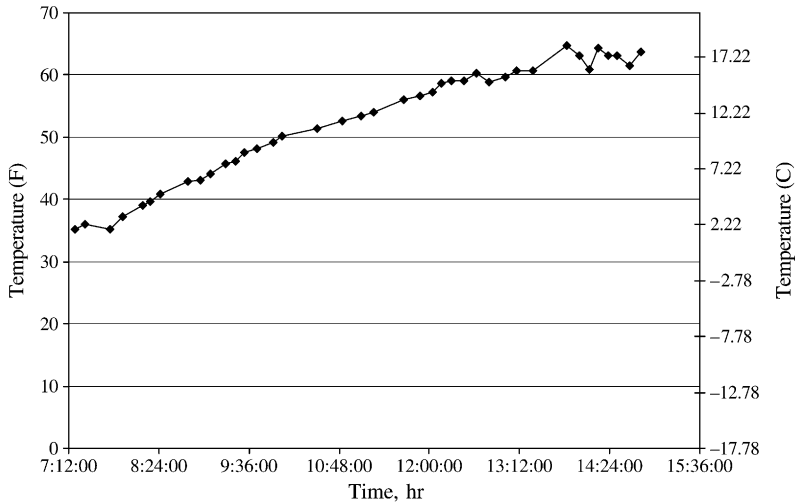
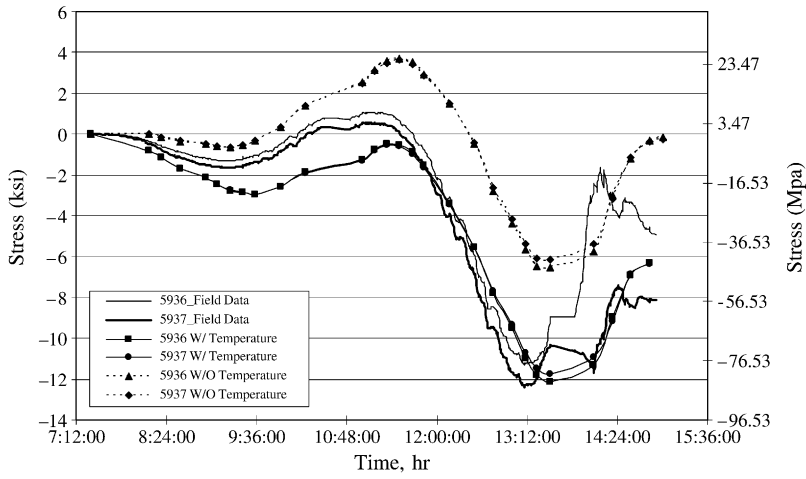


Fig. 8. Measured temperature variation during deck pour.

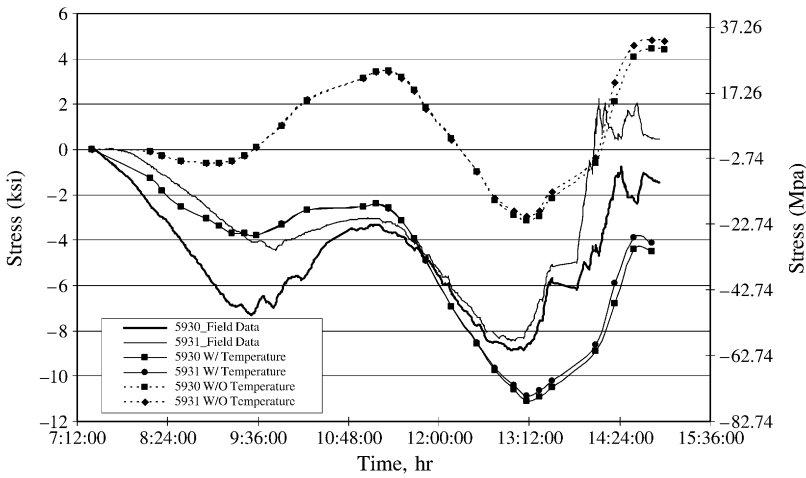
Table 1

Comparison between numerical and field flange stresses, pinned and roller supports

| Location | | Extreme 1 | | | Extreme 2 | | | Extreme 3 | | |
|----------|------|-------------|------------------------|---------------------|-------------|------------------------|---------------------|-------------|------------------------|---------------------|
| | | Field (ksi) | Roller (ksi) (% diff.) | Pin (ksi) (% diff.) | Field (ksi) | Roller (ksi) (% diff.) | Pin (ksi) (% diff.) | Field (ksi) | Roller (ksi) (% diff.) | Pin (ksi) (% diff.) |
| G1A | 5936 | -1.304 | -0.308 76 | -0.629 52 | 1.051 | 2.259 -115 | 3.544 -237 | -10.705 | -6.068 43 | -6.575 39 |
| | 5937 | -1.621 | -0.286 82 | -0.624 61 | 0.532 | 2.230 -319 | 3.516 -561 | -11.778 | -5.780 51 | -6.443 45 |
| | 5938 | -1.961 | 0.325 117 | 0.035 102 | -8.356 | -2.392 71 | -0.177 98 | -3.011 | 6.339 311 | 3.788 226 |
| G1B | 5933 | -1.281 | -0.159 88 | -0.561 56 | -1.669 | 1.203 172 | 3.165 290 | -8.113 | -3.236 60 | -2.855 65 |
| | 5934 | -0.024 | -0.161 -576 | -0.562 -2267 | -3.258 | 1.192 137 | 3.157 197 | -9.494 | -3.076 68 | -2.798 71 |
| | 5935 | -1.642 | 0.171 110 | 0.002 100 | -5.656 | -1.282 77 | 0.004 100 | -4.845 | 3.376 170 | 1.977 141 |
| G5A | 5931 | -6.886 | -0.168 98 | -0.618 91 | -3.356 | 1.575 147 | 3.363 200 | -8.722 | -3.983 54 | -3.003 66 |
| | 5930 | -3.553 | -0.164 95 | -0.616 83 | -3.057 | 1.569 151 | 3.365 210 | -8.286 | -3.807 54 | -3.085 63 |
| | 5932 | -0.826 | 0.177 121 | 0.013 102 | -4.672 | -1.675 64 | -0.067 99 | -3.770 | 4.160 210 | 2.217 159 |



(a) G1A.



(b) G5A.

Fig. 9. Experimental and numerical bottom flange stress variations, for G1 and G5, including temperature.

premature setting of the deck. However, recent research has shown that the development of composite action in steel–concrete systems with deck retarding agents can occur [40]. Therefore, the effects of premature composite action on the response of the system during construction were of interest.

Incorporation of the effects of formation of composite action during progression of the pour was examined through modifications to the concrete modulus for portions of the structure. Since time-dependent data regarding the concrete modulus was unavailable, incorporation of time-dependent modulus effects was conservatively accomplished as shown in Fig. 10. The modulus of elasticity was increased to its full value for portions

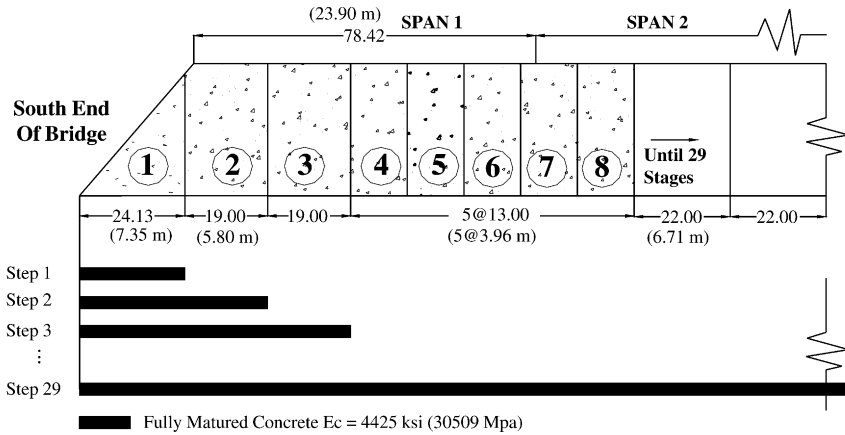


Fig. 10. Incorporation of the time-dependent modulus into numerical models.

of the span as the pour progressed with the entire pour being divided into 29 steps. As the pour progressed, previous deck sections were assigned the fully matured concrete stiffness to simulate a fully cured section.

Results from the analyses that included the effects of the formation of composite action are shown in Fig. 11(a) and (b). These plots indicate that incorporation of the change in the modulus and the subsequent incorporation of composite action has some small beneficial effects on the accuracy of the numerical predictions over a model that ignores these effects. The figures show that an improvement of approximately 3% was achieved by incorporating a variable concrete stiffness.

6.4. Combination of calibration results

A final calibration step involved examining the cumulative effects of incorporating the temperature changes and the time-dependent modulus modifications into the model with the chosen boundary conditions. This comparison provided some insight into the total improvement in modeling accuracy that would be achieved. Results from this analysis, which included temperature and composite action, are shown in Fig. 12(a) and (b) and are compared to field data and results from the original analysis that did not include temperature and time-dependent modulus effects. These figures show an appreciable improvement in behavioral predictions for a model including both temperature and modulus effects when compared to the original model, with differences between measured and predicted strains being reduced from 74% to 19%.

7. Pour sequencing study

At the completion of the calibration phase, girder stresses and deflections generated from the original deck placement method (case (a) from Fig. 1) were examined numerically and compared against a method that placed the concrete parallel to the skew (case (b)

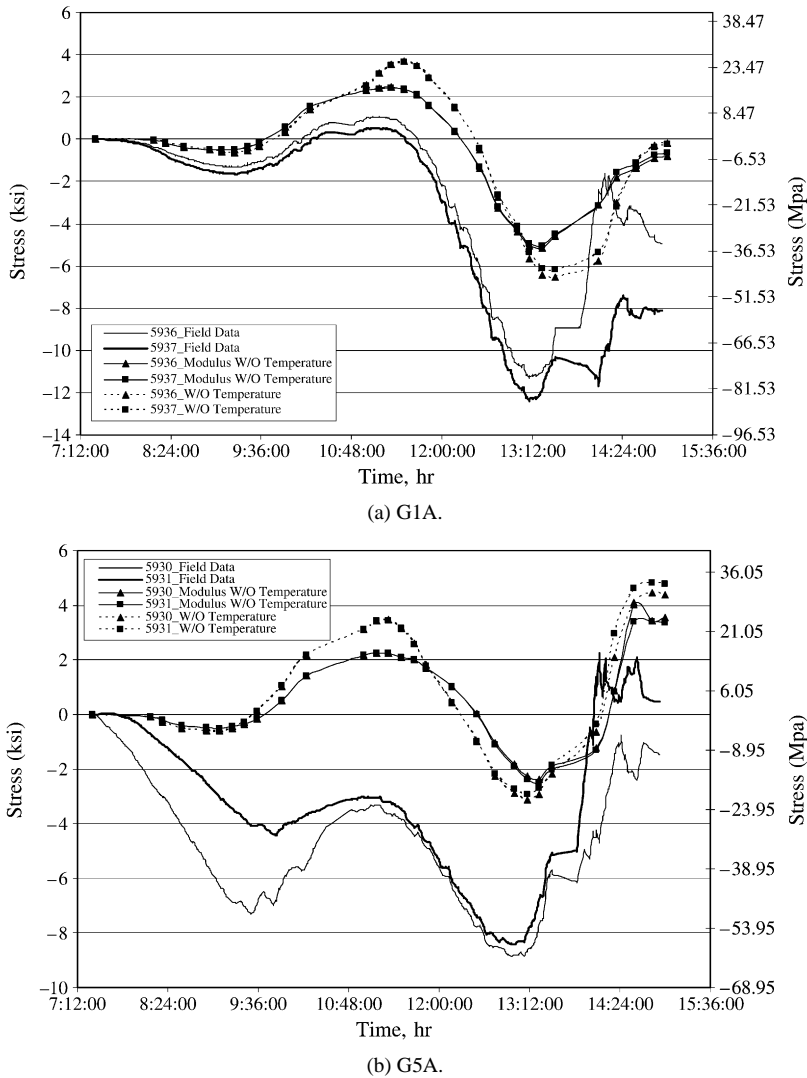
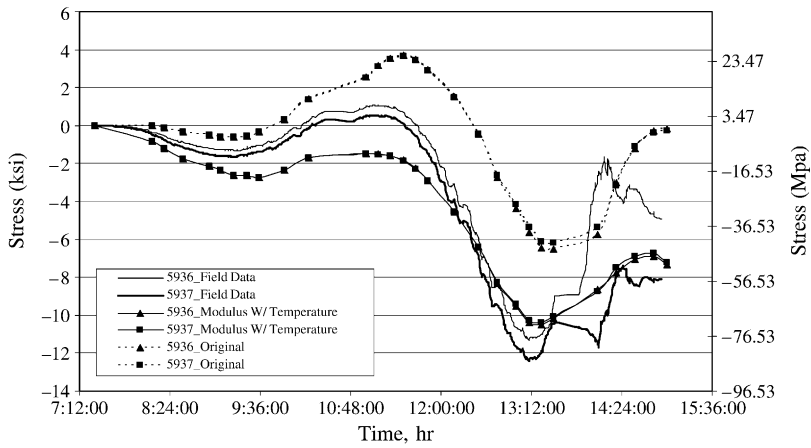


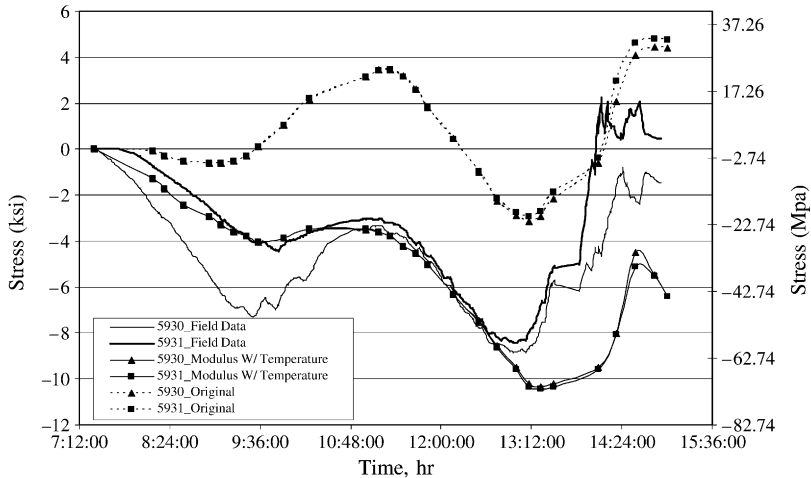
Fig. 11. Experimental and numerical bottom flange stress variations, for G1 and G5, including a time-dependent modulus.

from Fig. 1). These comparisons were used to establish whether one method resulted in reduced stresses and deformations being induced into the structure during the deck pour.

For each of these analyses, a total of 29 separate sequential steps were used to apply the steel and wet concrete loads to the structure. The first step represented the self-weight of the steel superstructure being activated while the remaining steps represented a portion of the wet concrete load being placed either perpendicular to the centerline or parallel to the skew.



(a) G1A.



(b) G5A.

Fig. 12. Experimental and numerical bottom flange stress variations, for G1 and G5, including temperature and a time-dependent modulus.

Fig. 13 provides a schematic detailing of how the wet concrete loads were applied for cases (a) and (b).

7.1. Study results

Fig. 14(a) and (b) detail bottom flange stress variations at G1B and G5A (Fig. 4) for cases (a) and (b) throughout the duration of the pour. As the deck is placed perpendicular to the roadway centerline, the bridge experiences the effect of differential girder deflections. The highest bottom flange stress differential observed between G1B and G5A is 4 ksi (27.6 MPa), a number that was representative of stress differentials observed at other

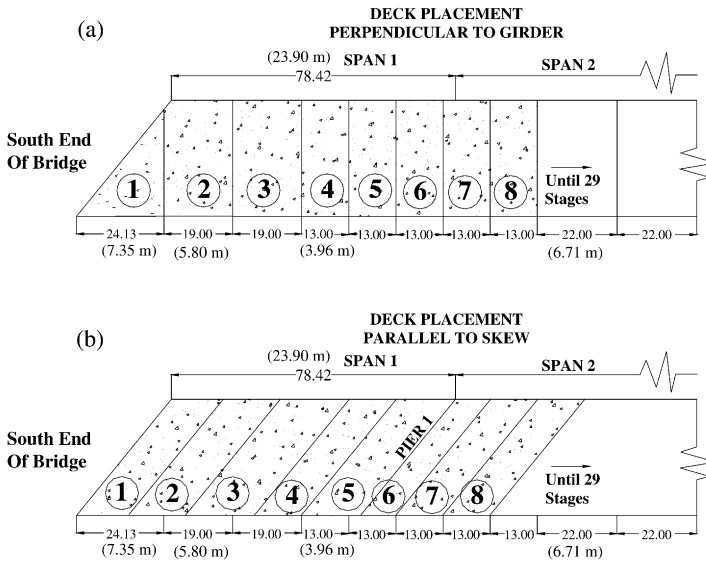


Fig. 13. The deck placement sequence: (a) perpendicular to the girder; (b) parallel to the skew.

locations within the superstructure and one that cannot be considered insignificant. These differences indicate global rotation of the bridge during the pour.

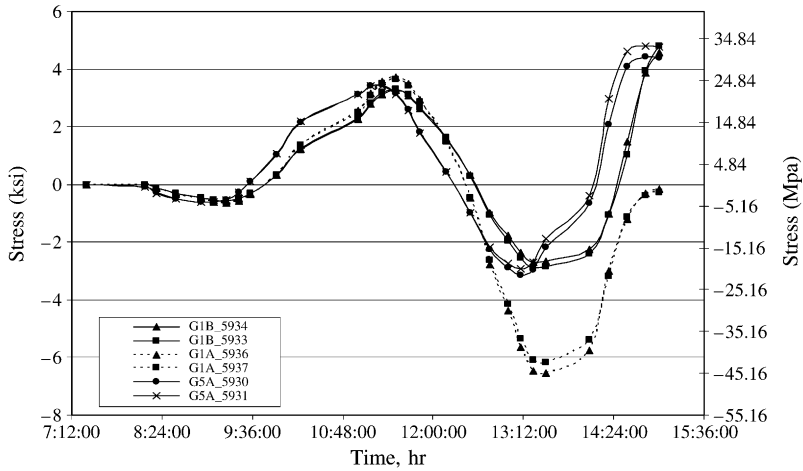
When the pour sequence was changed to being parallel to the skew, the maximum stress differentials observed between G1B and G5A were reduced to 0.42 ksi (2.9 MPa). This reduction indicated that only minor girder rotation was occurring as the pour progressed.

The influence of deck placement techniques on superstructure 2 response is further reinforced in Fig. 15(a) and (b), where vertical girder displacements are compared at G1B and G5A as the pour progresses. Fig. 15(a) indicates a maximum differential deflection of 0.57 in. (14.5 mm) occurring at around the 14th hour between G1A and G5A, indicating some rotation of the superstructure. Fig. 15(b) indicates differential deflection between G1A and G5A of 0.04 in (0.91 mm), indicating that there is an insignificant skew effect for deck placement parallel to the skew.

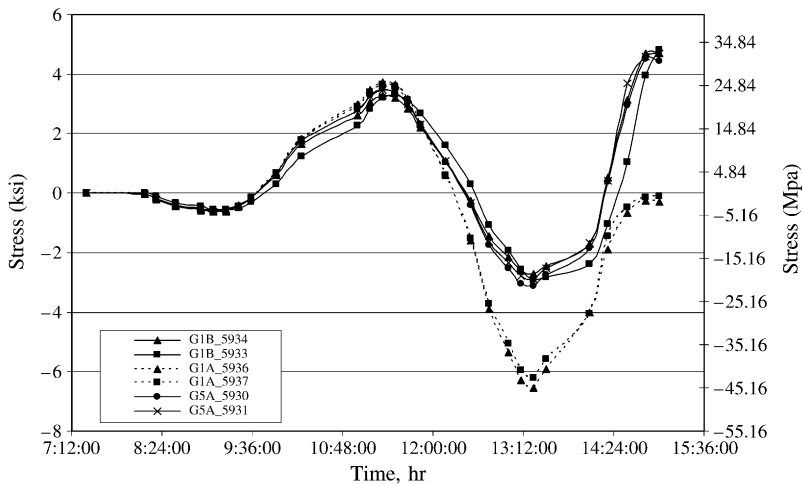
8. Conclusions

A finite element model was developed to study girder response during concrete deck placement for a continuous, skewed, steel, girder bridge. This model was calibrated against data recorded field monitoring of the structure’s response during the actual deck pour.

During calibration, it was recognized that field data sustained an increasing, superimposed compressive effect during deck placement that was not reproduced in the numerical models. Replication of this effect in the numerical models was attempted through incorporation of air temperature and time-dependent concrete stiffness



(a) Deck placement perpendicular to the centerline.

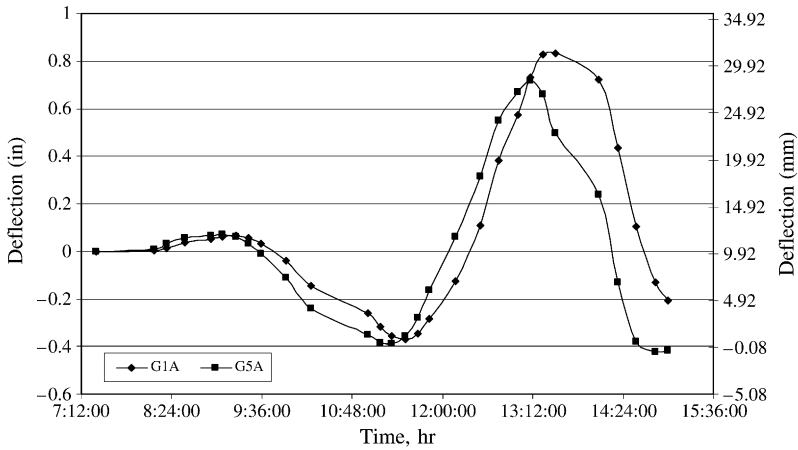


(b) Deck placement parallel to the skew.

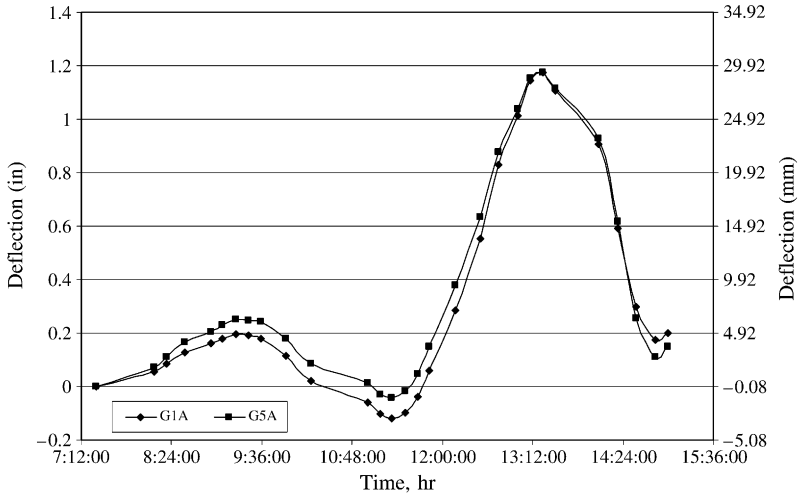
Fig. 14. Numerical model bottom flange stress variations.

variations. Incorporation of these aspects during model calibration steps indicated that:

1. Extreme changes in temperature during placement of the deck were of importance when attempting to accurately predict stress states in the superstructure at completion of the pour.
2. Incorporation of time-dependent concrete modulus effects and the subsequent formation of premature composite action were of minor importance when attempting to accurately predict stress states in the superstructure at completion of the pour.



(a) Deck placement perpendicular to the centerline.



(b) Deck placement parallel to the skew.

Fig. 15. Numerical model girder vertical displacements.

In addition, a numerical study investigating the effects of placing the wet concrete (1) perpendicular to the girders and (2) parallel to the skew was completed. These studies indicated that attempts to place the deck parallel to the skew would provide reduced differential deflections and stresses across the superstructure of the bridge that was studied. However, for this continuous structure the reductions were relatively small. Previous work by one of the authors [41] indicates that deck placement parallel to the skew for simply supported, steel structures with skew angles similar to those for the bridge studied herein provides a beneficial reduction of deformations and stresses that can result during construction. The combined results from that study and the current work indicate that,

while continuity can possibly reduce the beneficial effects that can result from placing wet concrete parallel to the skew, bridge designers and builders should consider this placement method as a viable option when developing construction plans for skewed, steel I-girder bridges. It should be noted that results reported herein were limited to a single structure; however, it can be inferred that they would be representative of the response of skewed, multi-beam, composite steel–concrete bridges. However, additional studies, both experimental and numerical, would need to be performed to assess the ranges of parameters (e.g. skew angle, number of spans, number of girders, boundary conditions) over which the conclusions obtained herein would be applicable.

Acknowledgements

The authors would like to acknowledge the Ohio Department of Transportation (ODOT) and the Federal Highway Administration's (FHWA) Innovative Bridge Research and Construction (IBRC) program for providing funding and technical assistance for this project.

References

- [1] Ebeido T, Kennedy JB. Girder moments in simply supported skew composite bridges. *Canadian Journal of Civil Engineering* 1996;23(4):904–16.
- [2] Gupta YP, Kumar A. Structural behavior of interconnected skew slab–girder bridges. *Journal of the Institution of Engineers (India)* 1983;64:119–24.
- [3] Aggour MS. Treatment of skew truss bridges as space frames. Thesis, Cairo University, Egypt; 1943.
- [4] Aggour MS. Theoretical and experimental study of space frame action and load distribution in square and skew bridges. Thesis, Cairo University, Egypt; 1947.
- [5] Ghali A. Analysis of continuous skew concrete girder bridge. In: *First international symposium on concrete bridge design*. American Concrete Institute; 1967.
- [6] Ghali A. Field measurement of end support reactions of a continuous multi-girder skew bridge. In: *Second international symposium on concrete bridge design*. American concrete institute; 1969. p. 260–71.
- [7] Hutter G. Skew and curved box-girders. Theory and research. In: *Proceedings of the seventh congress. International Association for Bridges and Structural Engineering*; 1964. p. 615–23.
- [8] Surana CS, Humar JL. Beam-and-slab bridges with small skew. *Canadian Journal of Civil Engineering* 1984;11(1):117–21.
- [9] Wasserman E, Azizinamini A, Pate H, Greer W. Making the grade. *Civil Engineering* 1998;68(4):69–71.
- [10] Wasserman E. Optimization of hps 70w applications. *ASCE Journal of Bridge Engineering* 2002;7(1):1–5.
- [11] Van Ooyen K. HPS success. *Modern Steel Construction* 2002;42(9):36–8.
- [12] American Iron and Steel Institute. HPS scoreboard, http://www.steel.org/infrastructure/bridges/high_performance/index.html; 2004.
- [13] Nickerson RL, Wright W. Weld parameter investigation for hps 70w steel. Presented at the HPS steering committee meeting; 1996.
- [14] Germanson T. Working with hps 70w steel. Presented at the 77th annual meeting of the transportation research board; 1998.
- [15] Nickerson RL. Tennessee department of transportation martin creek bridge, hps 70w steel fabrication and erection report and weld parameter study number 4. Presented at the HPS steering committee meeting; 1997.
- [16] Earls CJ, Shah BJ. High performance steel girder compactness. *Journal of Constructional Steel Research* 2002;58:859–80.
- [17] Green PS, Sause R, Ricles JM. Strength and ductility of hps flexural members. *Journal of Constructional Steel Research* 2002;58:907–41.

- [18] Yakel AJ, Mans P, Azizinamini A. Flexural capacity and ductility of hps-70w bridge girders. *Engineering Journal* 2002;39(1):38–51.
- [19] Barker MD, Schrage SD. High performance steel: design and cost comparisons. *Modern Steel Construction* 2000;46(6):35.
- [20] Burke MP. Semi-integral bridges: movements and forces. *Transportation Research Record: Journal of the Transportation Research Board* 1994;1460:1–7.
- [21] Abendroth RE, Greimann LF. A rational design approach for integral-abutment bridge piles. *Transportation Research Record: Journal of the Transportation Research Board* 1989;1223:12–23.
- [22] Ashour M, Norris G. Modeling lateral soil–pile response based on soil–pile interaction. *Journal of Geotechnical and Geoenvironmental Engineering* 2000;126(5):420–8.
- [23] Lehane BM, Keogh DL, O'Brien DJ. Simplified elastic model for restraining effects of backfill soil on integral bridges. *Computers and Structures* 1999;73(1–5):303–13.
- [24] Dicleli M. Simplified model for computer-aided analysis of integral bridges. *ASCE Journal of Bridge Engineering* 2000;5(3):240–8.
- [25] Hulsey JL, Emanuel JH. Environmental stresses in flexibility supported bridges. *Transportation Research Record: Journal of the Transportation Research Board* 1978;664:262–70.
- [26] Greimann LF, Yang PS, Wolde-Tinsae AM. Nonlinear analysis of integral abutment bridges. *ASCE Journal of Structural Engineering* 1986;112(10):2263–80.
- [27] Mourad S, Tabsh SW. Pile forces in integral abutment bridges subjected to truck loads. *Transportation Research Record: Journal of the Transportation Research Board* 1998;1633:77–83.
- [28] Nicholoso BA. Effects of temperature, shrinkage and creep on integral bridges. In: *Proceedings of the Henderson Colloquium towards joint free bridges*; 1994. p. 33.
- [29] Burke MP. The design of integral bridges. *Concrete International* 1996;15(6):37–42.
- [30] Girton DD, Hawkinson TR, Greimann FF. Validation of design recommendations for integral-abutment piles. *ASCE Journal of Structural Engineering* 1991;117(7):2117–34.
- [31] Wolde-Tinsae AM, Greimann LF. General design details for integral abutment bridges. *Civil Engineering Practice* 1988;3(2):7–20.
- [32] Husain I, Bagnariol D. Performance of integral abutment bridges. Ministry of Transportation Bridge Office Report BO-99-04, Ontario, Canada; 2000.
- [33] Oesterle RG, Refai TM, Volz JS, Scanlon A, Weiss WJ. Jointless and integral abutment bridges analytical research and proposed design procedures. Construction Technology Laboratories, Inc.; 1998.
- [34] Alampalli S, Yannotti AP. In-service performance of integral bridges and jointless decks. *Transportation Research Record: Journal of the Transportation Research Board* 1998;1624:2–7.
- [35] Ingram EE, Burdette EG, Goodpasture DW, Deatherage JH. Evaluation of applicability of typical column design equations to steel H-piles supporting integral abutments. *Engineering Journal* 2003;40(1):50–8.
- [36] Emerson M. Thermal movements of concrete bridges—field measurements and methods of prediction. Publication SP—American Concrete Institute; 1981. p. 77–102.
- [37] Thippeswamy HK, Ganga Rao HVS. Analysis of in-service jointless bridges. *Transportation Research Record: Journal of the Transportation Research Board* 1995;1476:162–70.
- [38] Lawver A, French C, Shield CK. Field performance of an integral abutment bridge. *Transportation Research Record: Journal of the Transportation Research Board* 2000;1740:108–17.
- [39] Laman JA, Linzell DG, Leighty CA, Fennema JL. Methodology to predict movement and stresses in integral abutment bridges. Pennsylvania Department of Transportation; 2003.
- [40] Topkaya C. Behavior of steel trapezoidal box girders during construction. Ph.D. thesis, Department of Civil Engineering, University of Texas at Austin; 2002.
- [41] Norton EK, Linzell DG, Laman JA. Examination of response of a skewed steel bridge superstructure during deck placement. *Transportation Research Record: Journal of the Transportation Research Board* 2003;1845:66–75.